Photosensitive properties of Schottky type photodiodes prepared by spin coating of isoniazid Schiff base thin film on p-Si

Ali Osman Tezcan[1] · Pınar Oruç[2] · Nihat Tuğluoğlu[3] · Serkan Eymur[3]

Abstract

In this study, a layer of isonicotinohydrazide and pyrene-based Schiff base (PyMIs) was formed on the front side of a p-Si semiconductor using the spin coating method, and an Al/PyMIs/p-Si/Al diode was fabricated. The *I-V* characteristics of the fabricated diode were measured under dark and from 20 to 100 mW/cm^2 illumination intensities for both forward and reverse bias. Diode parameters, including saturation current (I_0), ideality factor (n), and barrier height (φ_b) were investigated for all measurements based on thermionic emission theory. The values n changed from 2.51 to 2.05, and the φ_b changed from 0.77 eV to 0.86 eV as light intensity increased from dark to 100 mW/cm^2. The series resistance (R_s) values of the diode were investigated using the modified Norde's function and Cheung's functions. An analysis of the forward $log\,(I) - log\,(V)$ plot of Al/PyMIs/p-Si (MOmS)-type diode specified the carrier transport domination by ohmic conduction in the lower bias regions, by the space-charge-limited current (SCLC) at medium bias regions and the trap-charge limit current (TCLC) transport mechanism at higher bias regions. The fabricated diode exhibited typical photodiode behavior with reverse current values increasing from 9.13×10^{-6} A to 1.05×10^{-4} A, respectively. Furthermore, $I - V$ characteristics illuminated from 20 to 100 mW/cm^2 were also studied, and they indicated that the Al/PyMIs/p-Si diode could operate in a photovoltaic regime.

Keywords Isoniazid · Schottky diode · Series resistance · Photodiode · Illumination intensity · Current voltage

✉ Nihat Tuğluoğlu
  nihat.tugluoglu@giresun.edu.tr

1   Department of Electricity and Energy, Şebinkarahisar Vocational School, Giresun University, Giresun, Turkey

2   Department of Physics, Faculty of Sciences, Gazi University, Ankara, Turkey

3   Department of Energy Systems Engineering, Faculty of Engineering, Giresun University, Giresun, Turkey

🌀 Springer

1 Introduction

Semiconductor-based diodes are extensively used in the energy sector due to their various applications. Metal/semiconductor (M/S) junctions are crucial for optoelectronic and electrical devices in semiconductor technology (Wilmsen 1985; Li 2012; Al-Ahmadi 2020üt 2020a). The broad investigation of various M/S contacts has led to a thorough understanding of the physics of M/S interactions. Due to their inexpensive cost and simplicity of fabrication, M/S contacts are used in a wide range of electrical equipment. Numerous investigations have demonstrated that the electrical and photoelectric characteristics of the M/S contacts interface can be enhanced by sandwiching the M and S between an insulating or interfacial layer consisting of organic semiconducting compounds (Hu et al. 2012; Kim et al. 2013; Ostroverkhova 2013; Lee et al. 2014; Kim and Lee 2015). The organic semiconducting layer affects device performance and enhances M/S contacts' electrical characteristics. For instance, organic molecules may result in changes (increases or decreases) in the ideality factor, barrier height, and series resistance of the diode (Karadeniz et al. 2005; Selçuk et al. 2007; Tezcan et al. 2021; Ulusan et al. 2021; Cavdar et al. 2023; Güçlü et al. 2023). Organic semiconducting compounds also help manage the redistribution of interface states or reduce chemical interaction at the surface (Sharma 2013). It is well known that when a drop potential crosses an interface layer in an M/S rectifier junction, the electric field of a semiconductor is altered.

Owing to their high dielectric constant, ability to store charge, and photostability, organic semiconducting materials are popular for developing semiconductor-based devices (Forrest and Thompson 2007; Roncali et al. 2014; Dey et al. 2015; Iftikhar et al. 2023). Recently, Schiff base compounds have emerged as interesting organic semiconductors due to their unique electrical and optical properties, among other organic compounds and polymers (Zhang et al. 2018; Dutta and Halder 2023; Halder 2023). Usually, Schiff base molecules are comparatively less reported in fabricating Schottky barrier diodes, probably because of the problem of frequent hydrolysis that can occur during device fabrication. Still, the uses of Schiff-base compounds in fabricating Schottky barrier diodes are vastly appreciated because the syntheses of Schiff-base compounds are quite straightforward, less expensive, and require less time (Fiat Varol et al. 2016; Sayin et al. 2017; Akın et al. 2021; Eymur et al. 2021; Uzun et al. 2021; Tuğluoğlu et al. 2023). However, although isoniazid and its derivatives have been utilized as linkers to create hybrid materials, there have been limited investigations on the impact of isoniazid-based Schiff base compounds as organic interfacial layers on the electronic parameters of Schottky devices (de Almeida et al. 2013; Mahmoudi et al. 2016; Roztocki et al. 2016a, Roztocki, Senkovska Roztocki et al. 2016bb, Sayin et al. 2017, Wu et al. 2017, Uzun et al. 2021). Thus, further research on the optical and electrical properties of Schiff-base compounds is still required to explore the potential applications of these compounds in optoelectronics.

Considering these worries, we synthesized PyMIs in our work, a Schiff base molecule derived from pyrene and isoniazid, in accordance with the literature (Fig. 1). Then, we fabricated the Al/PyMIs/p-Si/Al structure. Through illumination-dependent *I-V* measurements, the electrical and photoelectrical properties of the manufactured diode were evaluated. The purpose of this study is to investigate the effect of PyMIs, an organic interfacial layer, on the main electronic parameters of Al/PyMIs/p-Si Schottky structures.

2 Experimental details

2.1 Synthesis of PyMIs

The synthesis of PyMIs, prepared as the literature procedure, is depicted in Fig. 1. As seen, a simple one-step condensation reaction between the isoniazid (1) and pyrene-1-carbaldehyde (2) gives PyMIs in good yield. The structure was confirmed using ^{1}H and ^{13}C spectroscopy (Sayin et al. 2017). ^{1}H NMR (400 MHz DMSO-d_6): δ 12.26 (s, 1H, NH), 9.54 (s, 1H, -CH=N), 8.82–8.87 (m, 3 H, ArH), 8.60 (d, 1H, $J=8.0$ Hz, ArH), 8.38–8.40 (m, 4 H, ArH), 8.27 (q, 2 H, $J=11.2$ Hz, ArH), 8.14 (t, 1H, $J=7.6$ Hz, ArH), 7.92–7.93 (m, 2 H, ArH). ^{13}C NMR (100 MHz, DMSO): δ 162.01, 150.92, 150.15, 148.36, 140.99, 132.64, 131.32, 130.60, 129.41, 129.30, 129.06, 127.88, 127.13, 127.07, 126.70, 125.36, 125.74, 124.62, 124.22, 122.85, 122.00.

2.2 Production of Al/PyMIs/p-Si/Al diode

The p-type Si crystal used for diode production has an orientation of (100), a thickness of 525 μm, and a resistivity of 1–20 Ω-cm. The p-Si crystal was cleaned with trichloroethylene, methanol, and acetone for 5 min, and afterward, the p-Si wafer was etched in the solution of HF:H$_2$O in the ratio of 1:10 for 1 min. Si crystal was rinsed with 5 L of deionized water and then dried in dry nitrogen gas. The aluminum (Al, 99.999% purity, 200 nm) metal sub-contact on the matte surface of silicon was evaporated by thermal evaporation method at 5×10^{-5} Torr and kept in an oven at 570 °C for 5 min in a nitrogen environment. After the operation of ohmic contact, the solution of CHCl$_3$:PyMIs (10 ml:10 mg) was made, and the CHCl$_3$:PyMIs solution was drop coated on p-Si crystal by spin coating technique with the 1500 rpm for 1 min. and kept a vacuum oven at 50 °C for 1 h. Finally, to form a rectifier contact on the photoactive layer, 200 nm Al metal was thermally deposited through a copper shadow mask at 5×10-5 Torr in a vacuum system. The MOmS diode contact area was 4.335×10^{-2} cm^2. Thus, Al/PyMIs/p-Si/Al MOmS Schottky type diode was produced, and the schematic diagram of the MOmS diode is illustrated in Fig. 2. The MOmS diode's room temperature *I-V* measurements were evaluated under various illumination conditions using
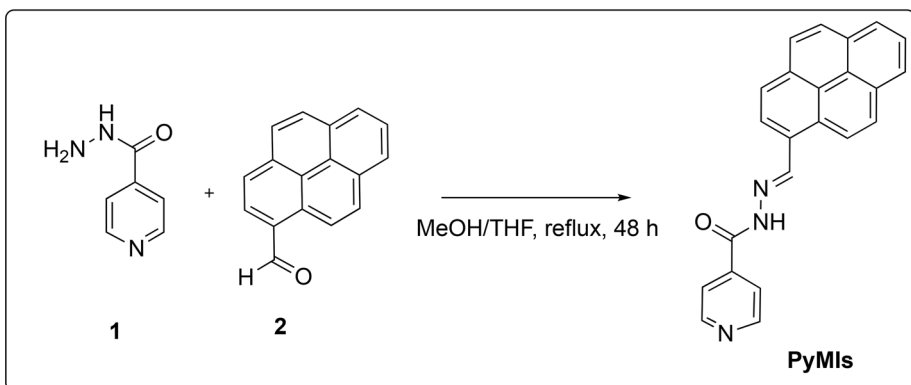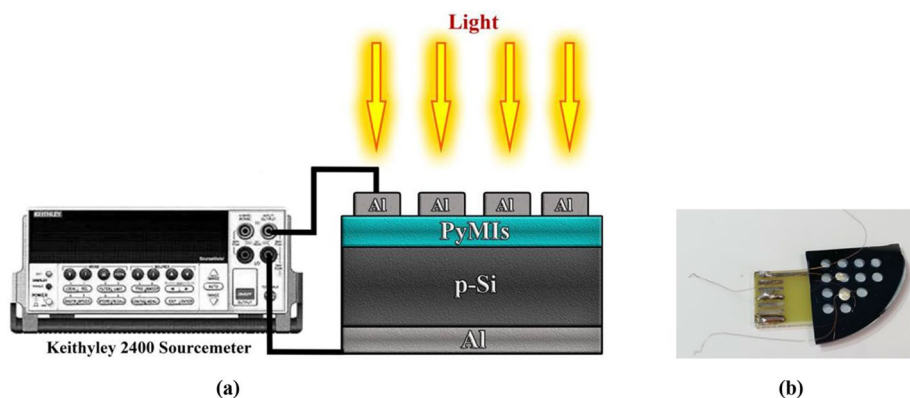

Fig. 1 Synthetic route to PyMIs

Fig. 2 **(a)** Schematic representation of Al/PyMIs/p-Si/Al device. **(b)** Physical photograph of Al/PyMIs/p-Si/Al device

a Fytronix Solar Simulator. All measurements were performed using a white light source in the 350–1100 nm wavelength range. To analyze the surface morphology of the PyMIs thin film, a Nano Magnetics atomic force microscope (AFM) was used.

3 Results and discussion

The ^{1}H-NMR and ^{13}C-NMR spectra of PyMIs are presented in Fig. 3 (a) and (b), respectively. It is understood that the synthesis of the compound has occurred due to the appearance of characteristic peaks belonging to the PyMIs structure in the NMR spectra. The iminium conjugation unit displays distinctive CH=N and -NH peaks at 9.54 and 12.26 ppm, respectively. By assigning the peaks at the region corresponding to the amide carbonyl carbon (C=O) and quaternary C of aromatic moieties, which appear at 162.01 ppm and between 140.99 and 150.92 ppm, respectively, C-NMR was also assigned to confirm the structure of PyMIs.

The synthesized PyMIs compound was computationally examined for its electronic structure, conductivity, and optimal molecular geometry using density-functional theory (DFT). The Gaussian 09 program suite was used to estimate the compound's ideal structural geometry, molecular static isotropic polarizability volume, molar volume, and assessments of its highest occupied molecular orbital (HOMO) and lowest occupied molecular orbital (LUMO) (Frisch et al. 2016). Frontier molecular orbitals were used to investigate various molecular properties like ionization potential, polarizability, electron affinity, electronegativity, excitability, hardness, softness, basicity, acidity, global reactivity, electrical and electronic charge transfers, and electronic transitions in chemical systems. Table 1 displays the calculated chemical descriptors derived from the simulated HOMO and LUMO level of the molecule in the gas phase using the DFT-B3LYP/6-311G(d,p) computational method.

Figure 4 (a) and 3 (b) illustrate the 2D and 3D AFM topographic surface images of the PyMIs thin film that was deposited onto the p-Si crystal by the spin coating method. The AFM analysis shown in Fig. 4 revealed a root mean square value of 11.38 nm, an average value of 32.54 nm, a ten-point height of 32.16 nm, a peak-to-peak value of 66.47 nm, and
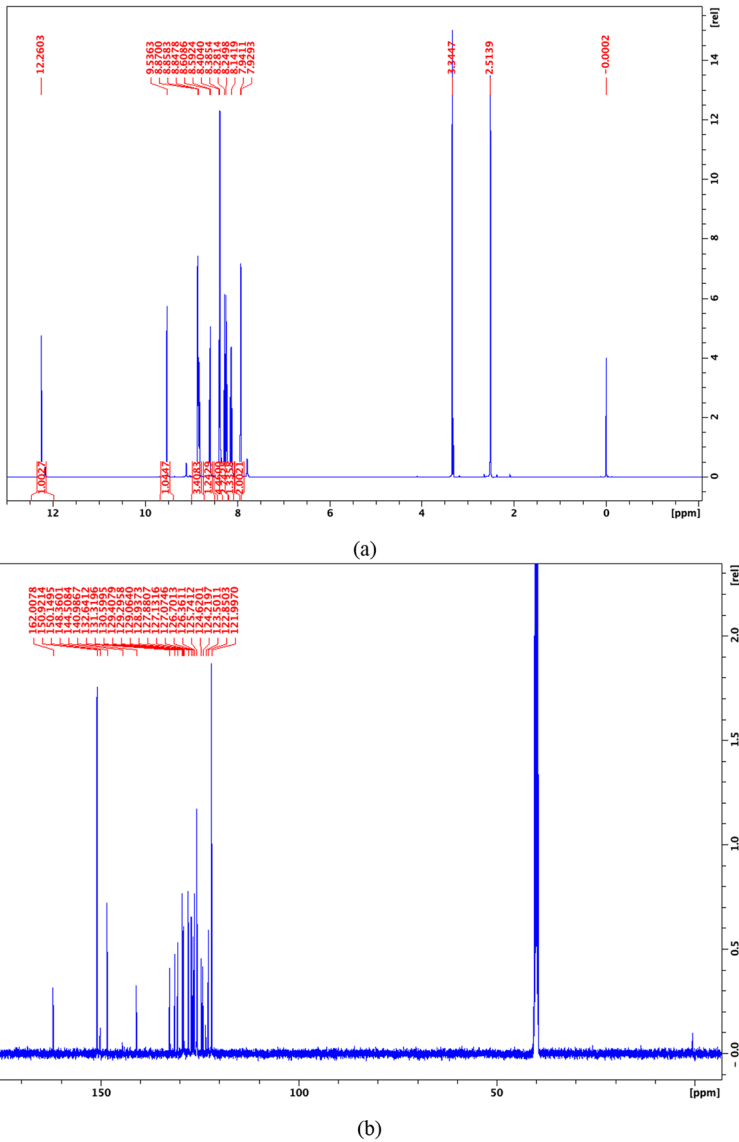
Fig. 3 (a) The ^{1}H-NMR spectrum, (b)^{13}C-NMR spectrum of PyMIs

an average roughness value of 8.85 nm. Research has shown that the surface roughness of thin films utilized as the interface layer has a major impact on a number of activities, including charge carrier collection, transfer, and transportation efficiency. The average roughness value of 8.85 nm indicates that the substrate surface was atomically flat. Additionally, a high level of flatness on the substrate surface results in a high-quality metal/semiconductor contact. The spin-coating method carried out the growth process of the PyMIs organic material on the Si substrate. A thorough literature review observed that the roughness values vary, and the results obtained fall within the accepted range in the literature (Khosravi et al.

Table 1 Computed some molecular descriptors based on the HOMO and LUMO energy values of the PyMIs

| Parameters	Value (eV)
E_{LUMO} (eV)	-2,437
E_{HOMO} (eV)	-5,727
Energy bandgap $|E_{HOMO} - E_{LUMO}|$	3,291
Ionization potential ($I = -E_{HOMO}$)	5,727
Electron affinity ($A = -E_{LUMO}$)	2,437
Chemical hardness ($h = (I-A)/2$)	1,645
Chemical softness ($z = 1/2h$)	0,304
Electronegativity ($\chi = (I+A)/2$)	4,082
Chemical potential ($\mu = -(I+A)/2$)	-4,082
Electrophilicity index ($w = \mu^2/2h$)	5,064
Maximum charge transfer index ($\Delta N_{max.} = -\mu/h$)	2,481

(a)

(b)
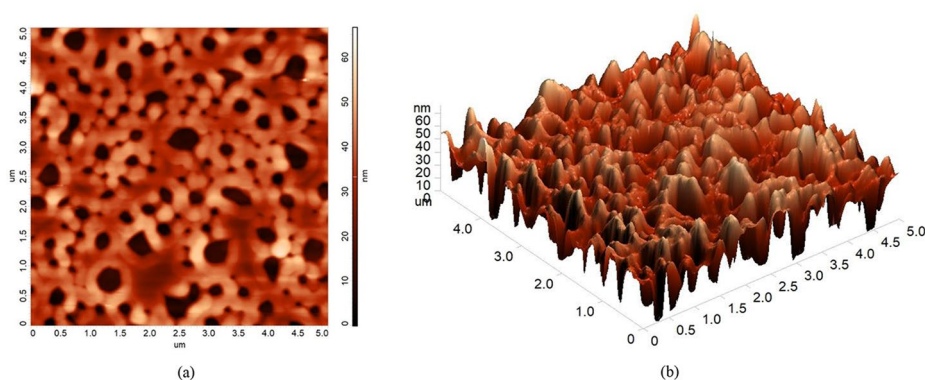
Fig. 4 (**a**) 2D, and (**b**) 3D AFM topographic surface images of PyMIs thin film on p-Si crystal

2020; Teldja et al. 2020; Özdal et al. 2021). Figure 5a shows a scanning electron microscope (SEM) image in cross-section. An average cross-sectional thickness of 50 nm is observed for the PyMIs organic compound on Si. The obtained SEM image of the surface depicted in Fig. 5b shows holes with a diameter of 100–300 nm are visible. This image also agrees with 3D AFM topographic surface images (Fig. 4. (a).

The *I-V* technique is one of the best-known approaches to studying the behavior of the Schottky diodes. Therefore, the semi-logarithmic *I-V* characteristic of the Al/PyMIs/p-Si/Al diode was investigated in the dark and different illumination intensities at room temperature and is shown in Fig. 6. As seen, the device had good rectification behavior. The rectification ratio was calculated in the dark and under 100 mW illumination intensity of 140 and 11, respectively. The rectification ratio of the Al/PyMIs/p-Si/Al diode was obtained by proportioning the reverse currents at ±2 V. Using thermionic emission theory (TE), the electrical characteristics of the Al/PyMIs/p-Si/Al diode have been determined. The relationship between current (*I*), voltage (*V*), and series resistance (R_s) can be written as follows based on TE (V ≥ 3kT/q) (Rhoderick 1982; Sze et al. 2021):

$$I = I_0 \left[exp \left(\frac{q(V - IR_s)}{nkT} \right) - 1 \right] \tag{1}$$
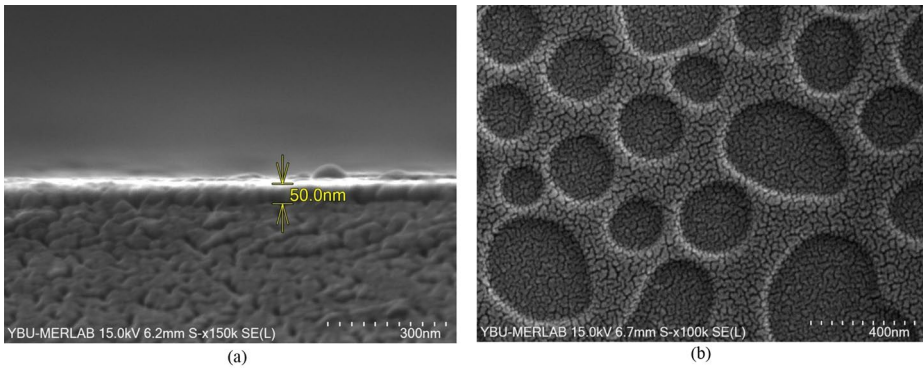
Fig. 5 SEM images of (**a**) cross-section, and (**b**) surface showing the thickness (50 nm) of PyMIs organic layer onto p-Si crystal

Fig. 6 Semilogarithmic *I-V* characteristics of Al/PyMIs/pSi/ Al Schottky diode under dark and various illumination intensities
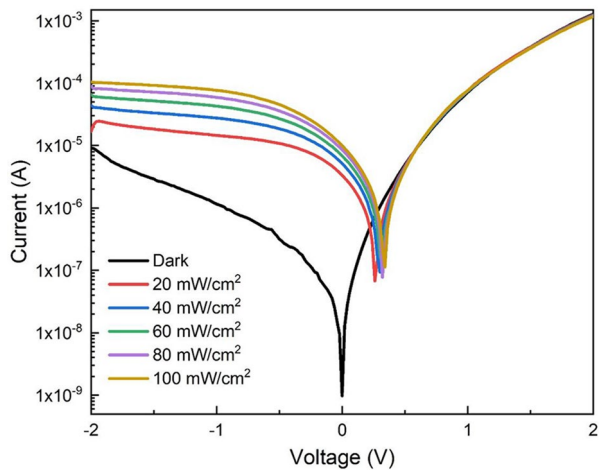
where I_0 is the saturation current, q is the electron charge, V is the applied voltage, and IR_s represent the voltage decrease across the series resistance (R_s) of the diodes, n is the ideality factor, k is the Boltzmann constant, T is the temperature in Kelvin. The saturation current I_0 is given by (Pakma et al. 2017; Banerjee et al. 2023):

$$I_0 = AA^*T^2 exp\left[-\frac{q\phi_b}{kT}\right] \tag{2}$$

where A is the diode contact area, A^* is the effective Richardson constant for p-Si ($A^* = 32$ AK^{-2} cm^{-2}), φ_b is the barrier height. If Eqs. 3 and 4 are arranged, the n and φ_b terms are written as,

$$n = \frac{q}{kT}\frac{dV}{d\left(lnI\right)} \tag{3}$$

and

$$\Phi_b = \frac{kT}{q} ln \left(\frac{AA^*T^2}{I_0} \right) \qquad (4)$$

The forward-bias *I-V* curve intercepts at zero voltage for each illumination intensity giving the values of I_0. The slope of the linear region of the *I-V* curves determines the values of *n*. In addition, φ_b values can be obtained from the intercept of the linear region of the *I-V* curves. Calculated values of n, φ_b, and I_0 are given in Table 2. The *n* value is equal to one for an ideal diode. Table 2 shows that the calculated *n* values for the Al/PyMIs/p-Si/Al diode are greater than one in the dark and under different illumination intensities. This is the typical behavior of diodes with Schottky barriers. The obtained *n* values greater than one may be due to interface states, barrier height inhomogeneity, and series resistance. As seen in Table 2, n and φ_b values were calculated to be 2.51 and 0.77 for dark, respectively. Also, *n* and φ_b values were found to be 2.05 and 0.86 for 100 mW/cm^2 illumination intensity, respectively. As can be seen, *n* and I_0 values decrease with increasing illumination intensity, whereas φ_b values increase with increasing illumination intensity. This behavior is a known situation for Schottky barrier diodes under illumination intensity. As can be observed, the diode's *n* values were greater than 1, indicating that its interface states, barrier inhomogeneity, surface states/traps, and series resistance cause it to behave differently from an ideal diode. Because more photogenerated charge carriers are produced when the device's interface is illuminated, the n values fell as the illumination level increased (Colinge and Colinge 2005; Hu et al. 2012; Li 2012). Similarly, under different light conditions, the P_3C_4MT polymer/n-Si heterojunctions diode was examined by Seymen et al. (Seymen and Karataş 2023). They found that the φ_b values increased as the light intensity increased while the *n* values fell linearly. Vivek et al. (2020) studied the properties and effect of the heterojunction using a MoO_3 nanoplate as an interlayer at the metal/semiconductor interface. According to their findings, the heterojunction's ideality factor and barrier height were 6.30 and 0.53 eV in the dark and 4.75 and 0.70 eV in the light, respectively (Vivek et al. 2020). Similar to these findings, ideality factor for the synthesized Al/PyMIs/pSi/Al approached more ideal values after light irradiation. It generally indicates less interfacial charge recombination and better homogeneity of Schottky junctions.

As known, combining two semiconductors with varying electron affinities, band gaps, and work functions to create a heterojunction diode results in discontinuities in the energy bands caused by the alignment of the Fermi level. Anderson's affinity rule states that when the free interfacial states and the vacuum level are perfectly aligned (no interfacial dipole), the discontinuities in the conduction band (E_c) are equal to the difference in electron affinities of the semiconductors (Anderson 1960). The valence band discontinuities (ΔE_v) are calculated as $\Delta E_v = \Delta E_g - \Delta E_c$, with ΔE_g being the variance in band gap between the two

Table 2 The values of *n*, I_0, and φ_b determined from *I-V* characteristics under dark and different illumination intensities

Illumination intensity (mW/cm^2)	n	I_0 (A) (x 10^{-9})	φ_b(eV)
0	2.51	20.1	0.77
20	2.44	3.67	0.81
40	2.42	1.67	0.83
60	2.28	1.51	0.84
80	2.21	1.01	0.85
100	2.05	0.6	0.86

semiconductors. The formula to determine the total built-in voltage, V_{bi}, is as follows (Sze 1981; El-Nahass et al. 2011):

$$V_{bi} = \Delta\Phi_{Si} - \Delta\Phi_{PyMIs} \tag{5}$$

where $\Delta\Phi_{Si}$ and $\Delta\Phi_{PyMIs}$ represents the silicon work function and the organic material work function, respectively. The built in potential can be calculated using an Eq. (6) (Sze 1981, Zeyada et al. 2015)

$$\varphi_b = V_{bi} + V_p \tag{6}$$

where V_p represents the potential difference between the Fermi level and the top of the valence band in the neutral region of p-Si (0.228 eV) (Sze 1981). When PyMIs' φ_b is assigned as 0.77 eV, V_{bi} is calculated as 0.452 eV and then Φ_{PyMIs} is obtained as 4.43 eV. Thus, the band profile of the Al/PyMIs/p-Si/Al heterojunction diode can be illustrated in Fig. 7.

The logarithmic graph of the *I-V* curve was drawn to analyze the conduction mechanisms of the prepared Al/PyMIs/p-Si/Al diode in the forward bias region. As seen in Fig. 8, there are three different transmission mechanisms that have different slopes. In region 1, the slope was determined to be close to 1. This means that currents and voltages increase linearly, and the conduction mechanism exhibits ohmic behavior. In region 2, the slope was determined close to 2, and so the current conduction mechanism can be explained by the space charge limited current (SCLC) (Akgül et al. 2021; Sze et al. 2021). In region 3, at high voltage levels, the slope was determined to be higher than 3.53. Therefore, the current conduction mechanism can be explained by the trap-charge limited current (TCLC) (Fujimoto et al. 2014).

The series resistance (R_s) is an important parameter that causes deviations in the ideal *I-V* characteristics of MOmS structure. The R_s, n, and φ_b values of the Al/PyMIs/p-Si/Al diode in the dark and under various illumination intensities were determined by the Cheung method from the Eqs. (7) and (8), which are rearranged forms of Eq. (1). Cheung's functions

Fig. 7 Schematic representation of the energy band diagram of the Al/PyMIs/p-Si/Al device
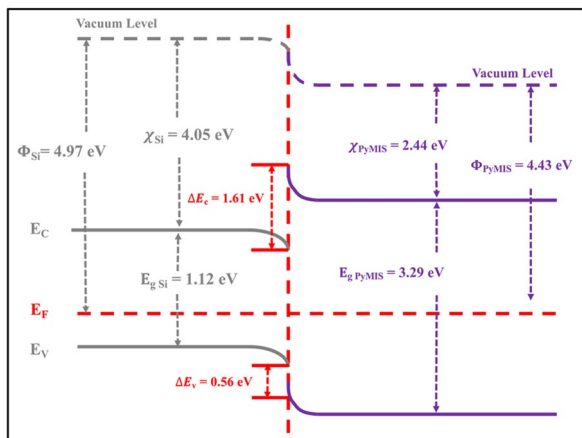
Fig. 8 The curves of $\ln I$ against $\ln V$ of the Al/ PyMIs /p-Si/Al diode at -2 V
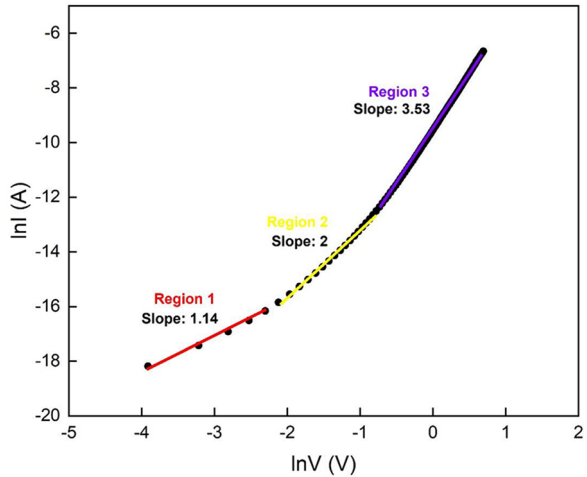
H(I) and dV/d ln(I) can be given as (Cheung and Cheung 1986, Moloi and Bodunrin 2023, Reddy et al. 2023):

$$H\left(I\right) = V - n\frac{kT}{q}ln\left(\frac{I}{AA^*T^2}\right) = n\varphi_b + IR_s \tag{7}$$

and

$$\frac{dV}{dlnI} = \frac{nkT}{q} + IR_s \tag{8}$$

The plots of dV/dln(I)-I and H(I)-I were generated in the dark and at different illumination intensities, as depicted in Fig. 9 (a) and (b). The values of R_s were determined from the slope of the H(I)-I and dV/dln(I)-I curves. The calculated R_s values are given in Table 3. The R_s values determined from the H(I) curve are 1.56 kΩ and 1.22 kΩ in dark and under 100 mW/cm^2 illumination intensity, respectively. The R_s values determined from the dV/dln(I) curve are 1.62 kΩ and 1.31 kΩ in dark and under 100 mW/cm^2 illumination intensity, respectively. As seen in Table 3, the decrease in R_s values with increasing illumination intensity can be attributed to the increase in free charge carriers with incident light absorption (Rideout 1978). In addition, the high R_s values obtained can be based to the interfacial state densities.

Another alternative approach used to determine R_s values of Al/PyMIs/pSi/Al diode is the Norde method. The Norde's functions can be given as (Norde 1979; Bodur et al. 2023; Omarbli and Imer 2023);

$$F\left(V\right) = \frac{V}{\gamma} - \frac{kT}{q}ln\left(\frac{I\left(V\right)}{AA^*T^2}\right) \tag{9}$$

and
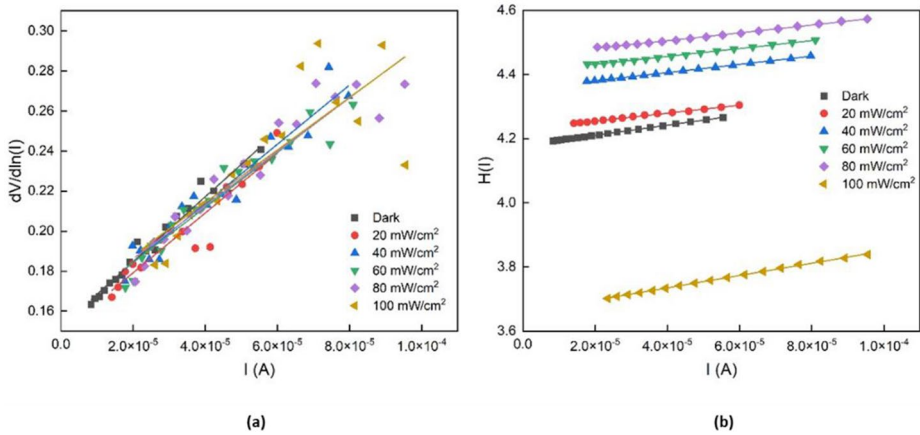
Fig. 9 The curves of (**a**) dV/d ln(I) versus I and (**b**) H(I) versus I of the Al/PyMIs/p-Si/Al diode for dark and various illumination intensities

Table 3 The values of R_s calculated from Cheung's and Norde's methods for dark and various illumination intensities

Illumination intensity (mW/cm²)	dV/dln(I) - I R_s (kΩ)	H(I) - I R_s (kΩ)	F(V) - V R_s (kΩ)
0	1.62	1.57	7.89
20	1.49	1.28	1.78
40	1.48	1.27	1.64
60	1.37	1.26	1.25
80	1.34	1.24	1.16
100	1.31	1.22	1.06

$$R_s = \frac{kT(\gamma - n)}{qI_{min}} \tag{10}$$

where γ is an integer that is greater than the ideality factor (n) values determined from I-V curves. I(V) is the current value determined from the *I-V* curve. After the F(V) functions were determined, F(V)-V plots were drawn under the dark and various illumination intensities as shown in Fig. 10. Devices with a high series resistance exhibit an inflection point in their F(V)-V function, as per Norde's theorem. However, when the series resistance is close to zero, no inflection point is observed. The F(V)-V curve in Fig. 10 displays the photovoltaic behavior of the generated diode, which increases within the range of 0.0-0.2 V. As it approaches the open-circuit voltage, the curve exhibits an inflection point due to the series resistance. The minimum values of F(V) -V plots have been determined. R_s values were determined from the minimum values of the F(V)-V plots according to Eq. 10. I_{min} is the current corresponding to $V_{min,}$ which is obtained from the minimum values of F(V) -V plots. The obtained R_s values in Norde's method are given in Table 3. The R_s values are 7.89 kΩ and 1.06 kΩ in dark and under 100 mW/cm² illumination intensity, respectively. As shown in Table 3, the calculated R_s values are decreasing with increasing illumination intensity. Also, R_s values calculated from the Cheung method and Norde method are approximately values to each other. The light-dependent behavior of the series resistor was also found

Fig. 10 Illumination dependence of F(V) versus V for Al/PyMIs/pSi/Al diode
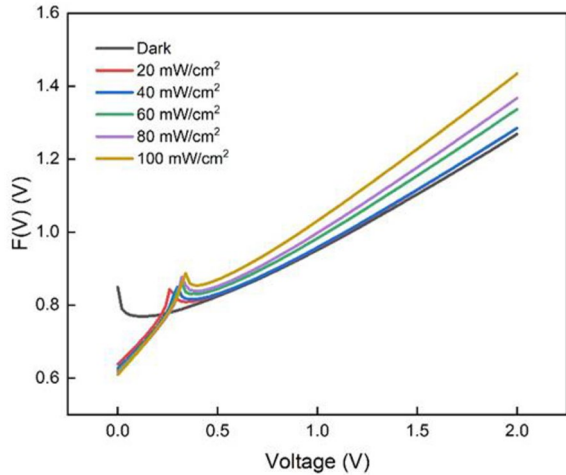
in similar studies. For example, in a study by Ghorai et al., aminoquinoline-based Schiff base ligands were used as interfacial layers for Al/semiconductor (MS) junctions. They found that Cheung's and Norde's functions were compatible with each other and that the series resistance values decreased after light in both cases (Ghorai et al. 2017). The series resistance values under dark and light conditions were determined to be 126 and 48 Ω, respectively, in a comparable study published by Chandra et al. on an ITO/fumaric acid coordination polymer and a pyridyl-hydrazide Schiff base/Al Schottky diode (Chandra et al. 2021). The observed decrease in series resistance when exposed to light, as reported earlier and confirmed in this work, demonstrates the potential use of these devices in electrical applications.

One of the key factors influencing the diode's performance in Schottky barrier diodes is the interface states, which are located between the semiconductor and the interface layer. The relationship between the interface state density (N_{ss}) and ideality factor (n) is expressed by Card and Rhoderick as (Card and Rhoderick 1971; Bengi et al. 2023; Çavdar et al. 2023):

$$N_{ss}(V) = \frac{1}{q}\left[\frac{\epsilon_i}{\delta_i}(n(V)-1) - \frac{\epsilon_s}{W_D}\right] \tag{11}$$

where ϵ_i and ϵ_s dielectric constant of interface and semiconductor, respectively. δ_i is the thickness of the interface layer, and W_D is the space charge region width. The relationship between the energy of the interface states (E_{ss}) and the top of the valence band energy of semiconductor (E_v) in p-type semiconductor is given as (Card and Rhoderick 1971):

$$E_{ss} - E_v = q(\Phi_e - V) \tag{12}$$

where q and φ_e are the electron charge and the effective barrier height, respectively. The curves of the values of N_{ss} versus E_{ss}-E_v for dark and various illumination intensities are shown in Fig. 11. The calculated N_{ss} values range from 7.14×10^{11} cm^{-2} eV^{-1} to 2.26×10^{11} cm^{-2} eV^{-1} and 5.17×10^{11} cm^{-2} eV^{-1} to 1.8×10^{11} cm^{-2} eV^{-1} for dark and 100 mW/cm^2

Fig. 11 N_{ss} vs. E_{ss}-E_v curves of Al/ PyMIs/p-Si/Al diode for dark and different illumination intensities
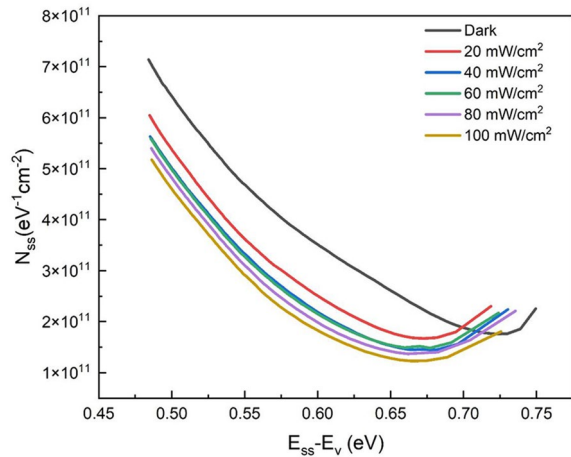
illumination intensity, respectively. It is seen that the N_{ss} values increase from the middle range of the Si semiconductor to the top of the valence band. Also, As seen in Fig. 11, N_{ss} values decrease with increasing illumination intensity. The decrease in N_{ss} values with the increase in illumination intensity shows that the interfacial layer behaves like a passivated material and therefore causes a decrease in N_{ss} values. The results of this study show that interfacial state densities (N_{ss}) are greatly affected by light exposure, as documented in the literature. Karataş et al. found that the N_{ss} values for the Al/n-CdO/p-Si device declined as the illumination intensity increased (Karataş and Yakuphanoğlu 2013). Likewise, in a study reported by Kaplan et al., the electrical measurement results of the Au/BODIPY-dye/n-Si/ In device showed decreased N_{ss} values with increasing illumination (Kaplan et al. 2021). The decrease in the N_{ss} values of the devices in this work and the above-mentioned studies with illumination is attributed to the discharge and charging of the interfacial states under the influence of illumination.

When the I-V characteristics of the Al/ PyMIs /p-Si/Al diode shown in Fig. 6 were examined, it was seen that it showed good rectification behavior. Also, the reverse bias current of the diode increases with increasing illumination intensity. This indicates the high light sensitivity of the diode, and it is known that this situation is a photodiode behavior (Colinge and Colinge 2005; Luque and Hegedus 2011; Schubert 2018). For this reason, the current density-voltage (J_{sc}-V) curves of the diode at dark and various illumination intensities were plotted to calculate the photodiode parameters and were shown in Fig. 12. The basic photovoltaic parameters open circuit voltage (V_{oc}) and short circuit current (I_{sc}) of diode were determined from the J_{sc}-V curves in Fig. 12. The open circuit voltage (V_{oc}) values are determined from where the current equals to zero in J_{sc}-V curves. In addition, the short circuit current (I_{sc}) values are determined from where the voltage equals to zero. The determined values are given in Table 4. According to this, V_{oc} values lightly increase, and I_{sc} values increase within a large limit with increasing illumination intensity. In addition, maximum voltage (V_{max}) and maximum current (I_{max}) values were determined from the largest area under the J_{sc}-V curve. It is also understood from studies in the literature that V_{oc} and J_{sc} values exponentially increase with incident light intensity. For example, in a study reported by İmer et al., a photodiode based on bromothymol blue dye was produced, and J_{sc} and V_{oc}

Fig. 12 Illumination intensity depen-
dent *J-V* curves of Al/PyMIs/p-Si/
Al diode
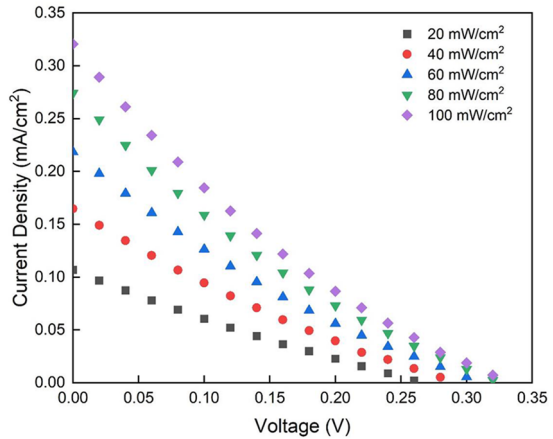
Table 4 Variation of photodiode parameters of Al/PyMIs/p-Si/Al Schottky diode depending on illumination intensity

Power (mW/cm^2)	V_{oc} (mV)	J_{sc} (mA/cm^2)	V_{max} (mV)	I_{max} (μA)	FF	P_{max}(mW/cm^2) (x 10^{-3})
20	260	0.1	120	1.64	22.5	6.25
40	280	0.16	140	2.23	21.5	9.92
60	300	0.22	140	3.00	20.4	13.3
80	320	0.27	140	3.80	19.3	16.9
100	320	0.32	140	4.44	19.3	19.7

values were calculated as 54.68 μA and 406 mV, respectively, under 100 mW/cm^2 light (Imer et al. 2016). At an illumination intensity of 40 mW/cm^2, these values were determined to be 14.69 μA and 347 mv, respectively. The consistent findings in this study and previous research suggest that the photosensitivity of these diodes is contingent on the intensity of the light, leading to the generation of electron-hole pairs by photons.

Additionally, other photovoltaic parameters, the values of maximum power (P_{max}) and fill factor (*FF*), are given as (Karataş and Berk 2022):

$$P_{max} = V_{max}I_{max} \tag{13}$$

and

$$FF = \frac{V_{max}I_{max}}{V_{oc}I_{sc}} \tag{14}$$

The values of P_{max} and *FF* under various illumination intensities are given in Table 4. According to this, P_{max} values increase as *FF* values decrease with increasing illumination intensity. This situation is an expected behavior for photodiodes.

Photosensitivity (*S*) is another important parameter in understanding the photosensitivity of Schottky barrier diodes. Photosensitivity (*S*) can be given as (Yahia et al. 2017; Darwish et al. 2022) :

$$S\,(\%) = \frac{I_{ph}}{I_{dark}} \times 100 \tag{15}$$

where I_{dark} and I_{ph} are dark current and generated photocurrent, respectively. Photosensitivity (S) values were calculated under the -2 V for each illumination intensity. Then, photosensitivity (S) versus the illumination intensity curves were drawn and shown in Fig. 13 (a). As seen in Fig. 13 (a), photosensitivity (S) values increase with increasing illumination intensity, and the diode of Al/PyMIs/p-Si/Al shows a good photosensitivity behavior.

Photoresponsivity (R) is another main parameter of light responsivity. Photoresponsivity (R) is expressed by the following equation. (Hendi 2015; Aslan et al. 2019; Akin et al. 2020):

$$R = \frac{I_{ph}}{P.A} \tag{16}$$

where A is the diode area, and P is the illumination intensity. The photoresponsivity (R) versus voltage (V) curves of Al/PyMIs/p-Si/Al diode for various illumination intensities were plotted and shown in Fig. 13 (b). As seen in Fig. 13 (b), the values of photoresponsivity (R) increase with increasing the bias voltage for each illumination intensity. This situation shows that the diode of Al/PyMIs/pSi/Al can be used to manufacture the photodiodes and photosensors in applications.

To analyze the photoconduction behavior of the Al/PyMIs/p-Si/Al Schottky Diode, the relationship $\ln I_{ph}$ and $\ln P$ was examined. The variation of the photocurrent (I_{ph}) dependency on illumination intensity can be given by the following equation (Bube 1992; Yahia et al. 2017):

$$I_{ph} = \gamma P^{\beta} \tag{17}$$

where γ is a constant, β is an exponent which is obtained from the slope of the $\ln I_{ph}$ versus $\ln P$ plot. The $\ln I_{ph}$-$\ln P$ curves were plotted for -2 V data and shown in Fig. 14. As seen in Fig. 14, the photocurrent increases with the illumination intensity. The values on this curve
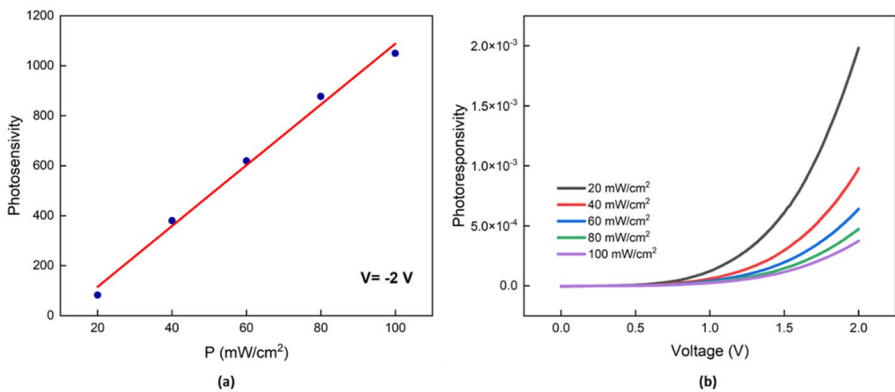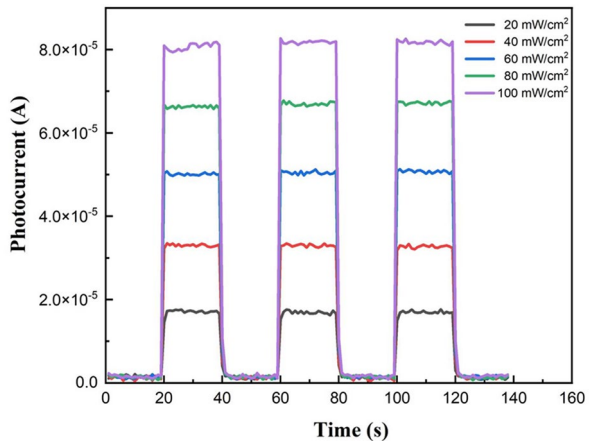

Fig. 13 The curves of (a) photosensitivity (S) vs. P and (b) photoresponsivity (R) vs. V for the Al/PyMIs/p-Si/Al diode

Fig. 14 The plot of $\ln(I_{ph})$ against $\ln(P)$ for Al/PyMIs/pSi/Al diode
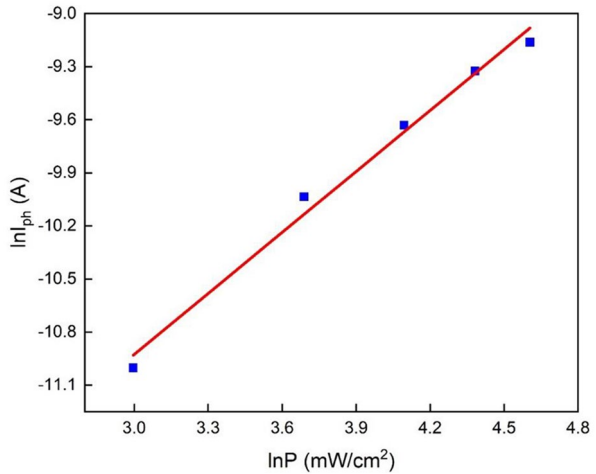
Fig. 15 Plots of Al/PyMIs/pSi/Al diode's photocurrent-time ($I_{ph} - t$) measurement

submit perfect linearity. The β value defines whether the recombination process is bimolecular or monomolecular. It also correlates with trap levels in the bandgap. The β value of Au/PyMIs/pSi diode has been calculated 1.15. This result displays a bimolecular recombination mechanism. Also, the value of β greater than 1 indicates the presence of low density unoccupied trap levels (Rose 1978; Arene and Baixeras 1984).

Figure 15 shows the produced diode's transient photocurrent behavior as a function of time. As shown in Fig. 15, the light intensity conditions used for the measurements were 20, 40, 60, 80, and 100 mW/cm². At −2 V, the measurements were conducted in various light intensities. The rapid fluctuations in photocurrents that occurred as the diode's light intensity increased demonstrated that the Al/PyMIs/pSi/Al Schottky diode had good photoconductive characteristics. The production of free charge carriers has contributed to the device's photocurrent rapidly increasing to its maximum level when the light was on. Rather, the lowest value of the photocurrent was recorded after the light was switched off. The reason for this behavior could be that charges are being trapped in the deep levels.

4 Conclusion

In summary, Al/PyMIs/p-Si/Al diode was prepared to show potential optoelectronic applications of PyMIs organic material. The thin film of PyMIs/p-Si diode was made by the spin coating method. The electrical and optical characteristics at the diode interface were explained by the current-voltage $(I - V)$ method under dark and different illumination intensities. The electrical conduction in the Al/PyMIs/p-Si Schottky diode was observed to take place by ohmic at low voltages, by SCLC at medium voltages, and by TCLC at higher voltages. All existing results reported that it was determined that the ideality factor and barrier height of the MOmS diode exhibited powerful illumination dependencies, in which the ideality factor decreases while barrier height increases as illumination intensity increases. It was found that the Al/PyMIs/p-Si/Al MOmS Schottky diode indicates a photovoltaic behavior with a J_{sc} of 0.32 mA cm^{-2} and V_{oc} of 320 mV for 100 mW/cm^2. In conclusion, as a result of the studied parameters of the Al/PyMIs/p-Si Schottky type photodiode, it can be evaluated that this photodiode, which is prepared easily and low cost, has the ability for photoelectrical device applications.

Data availability No datasets were generated or analysed during the current study.

Declarations

Competing interests The authors declare no competing interests.

References

Akgül, F.D., Eymur, S., Akın, Ü., Yüksel, Ö.F., Karadeniz, H., Tuğluoğlu, N.: Investigation of Schottky emission and space charge limited current (SCLC) in Au/SnO2/n-Si Schottky diode with gamma-ray irradiation. J. Mater. Sci. - Mater. Electron. **32**, 15857–15863 (2021)

Akin, U., Yuksel, O.F., Tasci, E., Tugluoglu, N.: Fabrication of a new hybrid Coronene/n-Si structure by using spin coating technique and its Photoresponse and Admittance Spectroscopy studies. Silicon. **12**, 1399–1405 (2020)

Akın, Ü., Sayın, S., Tuğluoğlu, N., Yüksel, Ö.F.: Investigation of Optical and Diode parameters of 9-[(5-Nitro-pyridin-2-Aminoethyl) Iminiomethyl]-Anthracene Thin Film. J. Electron. Mater. **50**, 2148–2156 (2021)

Al-Ahmadi, N.A.: Metal oxide semiconductor-based Schottky diodes: A review of recent advances. Mater. Res. Express. **7**, 032001 (2020)

Anderson, R.L.: Germanium-Gallium Arsenide heterojunctions [Letter to the editor]. IBM J. Res. Dev. **4**, 283–287 (1960)

Arene, E., Baixeras, J.: Steady-state photoconductivity and recombination process in sputtered hydrogenated amorphous silicon. Phys. Rev. B. **30**, 2016–2025 (1984)

Aslan, F., Esen, H., Yakuphanoglu, F.: The effect of coumarin addition on the electrical characteristics of Al/ Coumarin:CdO/p-Si/Al photodiode prepared by drop casting technique. Optik **197**, (2019)

Banerjee, A., Chakraborty, P., Chowdhury, J.R.: Aluminium/2-hydroxybenzaldehyde phenylhydrazone/aluminium organic MSM diode: An electrical and optoelectronic study. J. Mater. Sci. - Mater. Electron. **34**, (2023)

Bengi, S., Yükseltürk, E., Bülbül, M.M.: Investigation of electrical characterization of Al/HfO2/p-Si structures in wide temperature range. J. Mater. Sci. - Mater. Electron. **34**, 189 (2023)

Bodur, M.C., Duman, S., Orak, I., Saritas, S., Baris, O.: The photovoltaic and photodiode properties of Au/ Carmine/n-Si/Ag diode. Opt. Laser Technol. **162**, 109251 (2023)

Bube, R.H.: Photoelectronic Properties of Semiconductors. Cambridge University Press Cambridge, Cambridge (1992)

Card, H.C., Rhoderick, E.H.: Studies of tunnel MOS diodes I. Interface effects in silicon Schottky diodes. J. Phys. D: Appl. Phys. **4**, 1589 (1971)

Cavdar, S., Izmirli, S., Koralay, H., Turan, N., Eymur, S., Tugluoglu, N.: Optoelectronic properties of Triphenylamine Organic Thin Film Layered Al/p-Si /TPA/Al Heterojunction for Photodiode Application. ECS J. Solid State Sci. Technol. **12**, (2023)

Çavdar, Ş., Izmirli, S., Koralay, H., Turan, N., Eymur, S., Tuğluoğlu, N.: Optoelectronic properties of Triphenylamine Organic Thin Film Layered Al/p-Si /TPA/Al Heterojunction for Photodiode Application. ECS J. Solid State Sci. Technol. **12**, 045001 (2023)

Chandra, A., Das, D., Castro, J.-O., Naskar, K., Jana, S., Frontera, A., Pratim Ray, P., Sinha, C.: Cd(II) coordination polymer of fumaric acid and pyridyl-hydrazide Schiff base: Structure, photoconductivity and theoretical interpretation. Inorg. Chim. Acta. **518**, 120253 (2021)

Cheung, S.K.: Cheung. Extraction of Schottky diode parameters from forward current-voltage characteristics. Appl. Phys. Lett. **49**, 85–87 (1986)

Colinge, J.-P., Colinge, C.A.: Physics of Semiconductor Devices. Springer Science & Business Media (2005)

Darwish, A.A.A., Qashou, S.I., El-Zaidia, E.F.M., Yahia, I.S., El-Bashir, B.O., Alatawi, R.A.S., Hamdalla, T.A., Alfadhli, S.: Electrical and photoelectrical properties of a vacuum-deposited MnClPc/n-Si heterojunction for photodiode application. Micro Nanostruct. **167**, 207239 (2022)

de Almeida, F.B., e Silva, F.H., Yoshida, M.I.: De Abreu and R. Diniz. An interpenetrated 2D coordination polymer: A candidate for gas adsorption of small molecules. Inorg. Chim. Acta. **402**, 60–68 (2013)

Dey, A., Singh, A., Das, D., Iyer, P.K.: Organic Semiconductors: A New Future of Nanodevices and Applications. Thin Film Structures in Energy Applications. S. Babu Krishna Moorthy. Cham, Springer International Publishing: 97–128. (2015)

Dutta, B., Halder, S.: Fabrication of Schottky Barrier Diodes Utilizing Schiff Base Compounds and Metal Complexes with Schiff Base Ligands. ChemistrySelect 8, e202301586 (2023)

El-Nahass, M.M., Metwally, H.S., El-Sayed, H.E.A.: Hassanien. Electrical and photovoltaic properties of FeTPPCl/p-Si heterojunction. Synth. Met. **161**, 2253–2258 (2011)

Eymur, S., Tuğluoğlu, N., Apaydın, A., Akın, Ü.: Yüksel. Illumination Dependent Electrical and Photovoltaic properties of Au/n-Type Si Schottky Diode with Anthracene-based NAMA interlayer. ECS J. Solid State Sci. Technol. **10**, 051001 (2021)

Fiat Varol, S., Sayin, S., Eymur, S., Merdan, Z., Ünal, D.: Optical performance of efficient blue/near UV nitropyridine-conjugated anthracene (NAMA) based light emitting diode. Org. Electron. **31**, 25–30 (2016)

Forrest, S.R., Thompson, M.E.: Introduction: Org. Electron. Optoelectron. Chem. Rev. **107**, 923–925 (2007)

Frisch, M.J., Trucks, G.W., Schlegel, H.B., Scuseria, G.E., Robb, M.A., Cheeseman, J.R.: (2016). Gaussian 16 Rev. C.01. Wallingford, CT.

Fujimoto, H., Potscavage, W.J., Edura, T., Adachi, C.: Analysis of electron traps formed in organic films with a sputtered cathode. Org. Electron. **15**, 2783–2791 (2014)

Ghorai, P., Dey, A., Brandão, P., Ortega-Castro, J., Bauza, A., Frontera, A., Ray, P.P., Saha, A.: The development of a promising photosensitive Schottky barrier diode using a novel cd(ii) based coordination polymer. Dalton Trans. **46**, 13531–13543 (2017)

Güçlü, C.S., Tanrikulu, E.E., Dere, A., Altindal, S., Azizian-Kalandaragh, Y.: A comparison of electrical characteristics of the Au/n-Si Schottky diodes with (ZnCdS:GO(1:1)) and (ZnCdS:GO(1:0.5)) doped PVP interlayer using current-voltage (I-V) and impedance-voltage (Z-V) measurements. J. Mater. Sci. - Mater. Electron. **34**, (2023)

Halder, S.: Development of electrical conductivity-based photosensitive switching devices using metal complexes with Schiff base ligands. Mater. Adv. **4**, 5033–5049 (2023)

Hendi, A.A.: Electrical and photoresponse properties of graphene oxide: ZnO/Si photodiodes. J. Alloys Compd. **647**, 259–264 (2015)

Hu, W., Bai, F., Gong, X., Zhan, X., Fu, H., Bjornholm, T.: Organic Optoelectronics. Wiley (2012)

Iftikhar, R., Khan, F.Z., Naeem, N.: Recent synthetic strategies of small heterocyclic organic molecules with optoelectronic applications: A review. Mol. Diversity (2023)

Imer, A.G., Tombak, A., Korkut, A.: Electrical and photoelectrical characteristic investigation of a new generation photodiode based on bromothymol blue dye. J. Phys: Conf. Ser. **707**, 012012 (2016)

Kaplan, N., Tasci, E., Emrullahoglu, M., Gökce, H., Tugluoglu, N., Eymur, S.: Analysis of illumination dependent electrical characteristics of α- styryl substituted BODIPY dye-based hybrid heterojunction. J. Mater. Sci. - Mater. Electron. **32**, 16738–16747 (2021)

Karadeniz, S., Tugluoglu, N., Sahin, M., Safak, H.: Series resistance calculation for Ag contacts on single crystal layered p-SnS and p-SnSe compound semiconductors in the wide temperature range. Microelectron. Eng. **81**, 125–131 (2005)

Karataş, Ş., Berk, N.: Performance of the illumination dependent electrical and photodiode characteristic of the Al/(GO:PTCDA)/p-Si structures. Opt. Mater. **126**, 112231 (2022)

Karataş, Ş., Yakuphanoğlu, F.: Effects of illumination on electrical parameters of Ag/n-CdO/p-Si diode. Mater. Chem. Phys. **138**, 72–77 (2013)

Khosravi, M., Seyfi, J., Saeidi, A., Khonakdar, H.A.: Spin-coated polyvinylidene fluoride/graphene nanocomposite thin films with improved β-phase content and electrical conductivity. J. Mater. Sci. **55**, 6696–6707 (2020)

Kim, T.-D, Lee, K.-S.: D-π-A conjugated molecules for Optoelectronic Applications. Macromol. Rapid Commun. **36**, 943–958 (2015)

Kim, G.H., Shao, L., Zhang, K.: Pipe. Engineered doping of organic semiconductors for enhanced thermoelectric efficiency. Nat. Mater. **12**, 719–723 (2013)

Lee, C.W., Kim, O.Y., Lee, J.Y.: Organic materials for organic electronic devices. J. Ind. Eng. Chem. **20**, 1198–1208 (2014)

Li, S.S.: Semiconductor Physical Electronics. Springer New York, NY (2012)

Luque, A., Hegedus, S.: Handbook of Photovoltaic Science and Engineering. Wiley (2011)

Mahmoudi, G., Afkhami, F.A., Jena, H.S., Nematollahi, P., Esrafili, M.D., Garczarek, P., Van Hecke, K., Servati Gargari, M.: Kirillov. Halide ion-driven self-assembly of zn(ii) compounds derived from an asymmetrical hydrazone building block: A combined experimental and theoretical study. New. J. Chem. **40**, 10116–10126 (2016)

Moloi, S.J., Bodunrin, J.O.: Characterisation of interface states of Al/p-Si Schottky diode by current-voltage and capacitance-voltage- frequency measurements. J. Mater. Sci. - Mater. Electron. **34**, 1712–1722 (2023)

Norde, H.: A modified forward I-V plot for Schottky diodes with high series resistance. J. Appl. Phys. **50**, 5052–5053 (1979)

Omarbli, S.A., Imer, A.G.: Modification in the electronic parameters of M/p-Si hybrid device by PSP functional dye interface with different contact metals (M:Ag, Cu, pd, sn). Synth. Met. **297**, 117396 (2023)

Ostroverkhova, O.: Handbook of Organic Materials for Optical and (Opto)Electronic Devices: Properties and Applications. Elsevier (2013)

Özdal, T., Chtouki, T., Kavak, H., Figa, V., Guichaoua, D., Erguig, H., Mysliwiec, J., Sahraoui, B.: Effect of Annealing temperature on morphology and optoelectronics properties of spin-coated CZTS Thin films. J. Inorg. Organomet. Polym. **31**, 89–99 (2021)

Pakma, O., Çavdar, S., Koralay, H., Tugluoglu, N., Yüksel, Ö.: Improvement of diode parameters in Al/n-Si Schottky diodes with coronene interlayer using variation of the illumination intensity. Phys. B. **527**, 1–6 (2017)

Reddy, V.R., Rani, A.U., Ashajyothi, S., Reddy, D.S., Kumar, A.A.: Annealing temperature effect on structural, electronic features and current transport process of Au/CoPc/undoped-InP MPS-type Schottky structure. J. Mol. Struct. **1294**, 136490 (2023)

Rhoderick, E.H.: Metal-semiconductor contacts. IEE Proc. I (Solid-State Electron. Devices). **129**, 1–14 (1982)

Rideout, V.L.: A review of the theory, technology and applications of metal-semiconductor rectifiers. Thin Solid Films. **48**, 261–291 (1978)

Roncali, J., Leriche, P., Blanchard, P.: Molecular materials for Organic Photovoltaics: Small is beautiful. Adv. Mater. **26**, 3821–3838 (2014)

Rose, A.: Concepts in Photoconductivity and Allied Problems. Krieger Publishing Co, Huntington, N. Y. (1978)

Roztocki, K., Jędrzejowski, D., Hodorowicz, M., Senkovska, I., Kaskel, S., Matoga, D.: Isophthalate–hydra-zone 2D zinc–Organic Framework: Crystal structure, selective adsorption, and tuning of Mechano-chemical Synthetic conditions. Inorg. Chem. **55**, 9663–9670 (2016a)

Roztocki, K., Senkovska, I., Kaskel, S., Matoga, D.: Carboxylate–Hydrazone Mixed-Linker Metal–Organic Frameworks: Synthesis, Structure, and Selective Gas Adsorption. Eur. J. Inorg. Chem. 4450–4456 (2016b) (2016)

Sayin, S., Varol, S.F., Merdan, Z., Eymur, S.: Synthesis of isoniazid substituted pyrene (PINHy), and inves-tigation of its optical and electrochemical features as tunable/flexible OLEDs. J. Mater. Sci. - Mater. Electron. **28**, 13094–13100 (2017)

Schubert, E.F.: Light-Emitting Diodes. E. Fred Schubert (2018)

Selçuk, A.B., Tugluoglu, N., Karadeniz, S., Ocak, S.B.: Analysis of frequency-dependent series resistance and interface states of In/SiO2/p-Si (MIS) structures. Phys. B. **400**, 149–154 (2007)

Seymen, H., Karataş, Ş.: Investigation of electrical, photodiode and photovoltaic properties of Au/SiO2/n-Si structures with GO and P3C4MT interface. Mater. Chem. Phys. **310**, 128449 (2023)

Sharma, B.: Metal-semiconductor Schottky Barrier Junctions and Their Applications. NY, Springer New York (2013)

Sze, S.M.: Physics of Semiconductor Devices. Wiley, New York (1981)

Sze, S.M., Li, Y., Ng, K.K.: Physics of Semiconductor Devices. Wiley (2021)

Teldja, B., Noureddine, B., Azzeddine, B., Meriem, T.: Effect of indium doping on the UV photolumines-cence emission, structural, electrical and optical properties of spin-coating deposited SnO2 thin films. Optik. **209**, 164586 (2020)

Tezcan, A.O., Eymur, S., Tasci, E., Emrullahoglu, M., Tugluoglu, N.: Investigation of electrical and photo-voltaic properties of Au/n-Si Schottky diode with BOD-Z-EN interlayer. J. Mater. Sci. - Mater. Electron. **32**, 12513–12520 (2021)

Tuğluoğlu, N., Pakma, O., Akın, Ü., Yüksel, Ö.F., Eymur, S., Sayın, S.: The double gaussian distribution of Inhomogeneous Barrier Heights in Au/NAMA/n-Si Schottky diodes. ECS J. Solid State Sci. Technol. **12**, 035005 (2023)

Türüt, A.: On current-voltage and capacitance-voltage characteristics of metal-semiconductor contacts. Turk. J. Phys. **44**, 302–347 (2020a)

Ulusan, A.B., Tataroglu, A., Altindal, S., Azizian-Kalandaragh, Y.: Photoresponse characteristics of Au/(CoFe2O4-PVP)/n-Si/Au (MPS) diode. J. Mater. Sci. - Mater. Electron. **32**, 15732–15739 (2021)

Uzun, K., Sayın, S., Tamer, Ö., Çevik, U.: Comparison of charge transport and opto-electronic properties of pyrene and anthracene derivatives for OLED applications. J. Mol. Model. **27**, 174 (2021)

Vivek, P., Chandrasekaran, J., Marnadu, R., Maruthamuthu, S.: Fabrication of illumination-dependent Cu/p-Si Schottky Barrier diodes by sandwiching MoO3 nanoplates as an interfacial layer via JNSP technique. J. Electron. Mater. **49**, 4249–4264 (2020)

Wilmsen, C.: Oxide/III-V Compounds Semiconductor Interfaces. Physics and Chemistry of III-V Compound Semiconductor Interfaces (1985)

Wu, Y., He, J., Wang, S., Zou, L., Wu, X.: Syntheses, crystal structure, and photocatalytic property of two new complexes of an unsymmetrical Schiff base ligand. Inorg. Chim. Acta. **458**, 218–223 (2017)

Yahia, I.S., Farag, A.A.M., Jafer, R., Iqbal, J., Zahran, H.Y., Chusnutdinow, S., Wojtowicz, T., Karczewski, G.: Electrical, photovoltaic and photosensitivity characteristics of p-ZnTe:N/CdTe:Mg/n-CdTe:I/GaAs for photodiode applications. Mater. Sci. Semicond. Process. **67**, 33–40 (2017)

Zeyada, H.M., El-Nahass, M.M., El-Menyawy, E.M.: El-Sawah. Electrical and photovoltaic characteristics of indium phthalocyanine chloride/p-Si solar cell. Synth. Met. **207**, 46–53 (2015)

Zhang, J., Xu, L., Wong, W.-Y.: Energy materials based on metal Schiff base complexes. Coord. Chem. Rev. **355**, 180–198 (2018)